Supplementary information for:

A multi-channel chip enabled synchronized reciprocating-flow of fluid for rapid, simultaneous, multiplex detection of inflammatory markers

Juanhua Li [†a], Zihan Xiao [†a], Tianyu Wu [a], Yiren Liu [a], Wenyong Zhang [b], Cuiping Zhou [*b], Yanqiong Su [cd], Hongrui Liang [a], Donglin Cao[*cd], Jianhua Zhou [*a]

a Key Laboratory of Sensing Technology and Biomedical Instruments of Guangdong Province, School of Biomedical Engineering, Shenzhen Campus of Sun Yat-sen University, Shenzhen, Guangdong, 518107, China.

b Department of Emergency, Nanfang Hospital, Southern Medical University, Guangzhou, 510515, China.

c The Affiliated Guangdong Second Provincial General Hospital of Jinan University, Guangzhou, 510317, China.

d The Second School of Clinical Medicine, Southern Medical University, Guangzhou, China.

† These authors contributed equally.

Correspondence: cpzhou2007@126.com (C. Zhou); caodl@126.com (D. L. Cao); zhoujh33@mail.sysu.edu.cn (J. H. Zhou); Tel./Fax: +86-20-3938-7890

Supplementary Notes

Note S1. Calculation of limit of detection (LOD)

The calculation of LODs in this manuscript followed the equation R1.

$$LOD = k \cdot C_b \cdot \sigma/\bar{I} \#(R1)$$

where the k is a constant, and its value depends on the distribution and confidence interval of the sample detection data; C_b is the lowest concentration of the sample detected in the concentration gradient of the standard curve; σ is the standard deviation of the data from the repeated detection of the sample with lowest concentration; $\bar{I}$ is the average value (color intensity) of the detection results of the sample with lowest concentration.

Firstly, we evaluated the normal distribution and confidence intervals of detection data of different inflammatory markers using the Shapiro Wilk test (**Fig. S11**).

The results indicated that, the detection data of CRP standard sample followed a normal distribution with a confidence interval of 99.7%. Therefore, the value of k was taken as 3, and the calculation formula of LOD was expressed as equation R2.

$$LOD_{CRP} = 3 \cdot C_b \cdot \sigma/\bar{I} \#(R2)$$

The detection data of PCT standard sample followed a normal distribution with a confidence interval of 99.7%. Therefore, the value of k was taken as 3 and the calculation formula of LOD was expressed as equation R3.

$$LOD_{PCT} = 3 \cdot C_b \cdot \sigma/\bar{I} \#(R3)$$

The detection data of IL-6 standard sample followed a normal distribution with a confidence interval of 99.7%. Therefore, the value of k was taken as 3, and the calculation formula of LOD was expressed as equation R4.

$$LOD_{IL-6} = 3 \cdot C_b \cdot \sigma/\bar{I} \#(R4)$$

The detection data of SAA standard sample followed a normal distribution with a confidence interval of 99.7%. Therefore, the value of k was taken as 3, and the calculation formula of LOD was expressed as equation R5.

$$LOD_{SAA} = 3 \cdot C_b \cdot \sigma / \bar{I} \quad \#(R5)$$

In this way, by substituting the corresponding value of C_b, σ and $\bar{I}$ into equations R2-R5, the LOD of each biomarker can be obtained.

Supplementary Figures

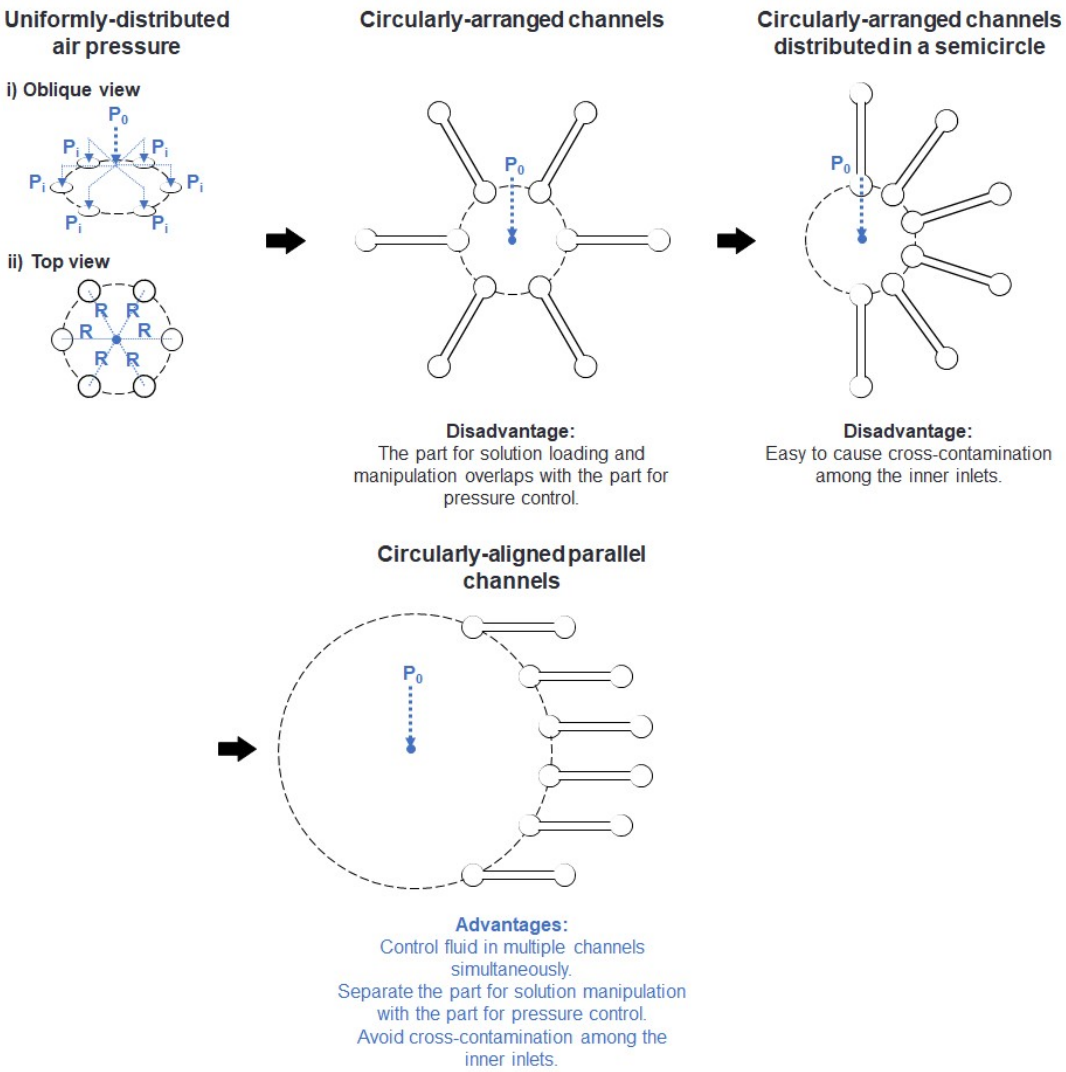

Fig. S1 The design concept of the CAPC chip.

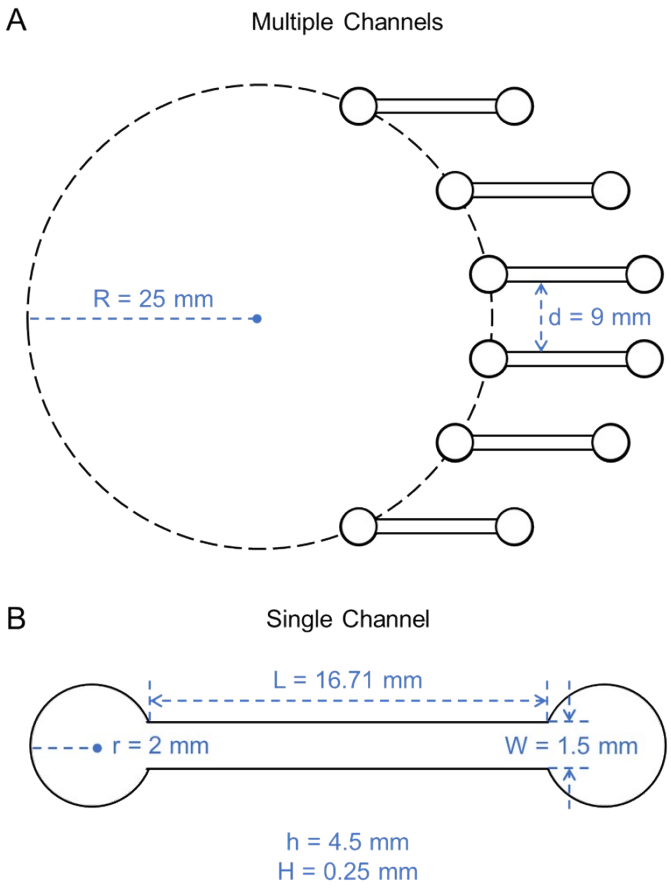

Fig. S2 The channel parameters and the layout distribution of the CAPC chip. (A) The layout distribution of multiple channels on the CAPC chip. The channels are arranged along the circumference of a circle with radius R, and the distance between each channel is d. (B) Top view and parameters of a single channel. r and h represent the radius and height of the cylindrical through-hole, respectively. L, W, and H represent the length, width, and height of the straight channel, respectively.

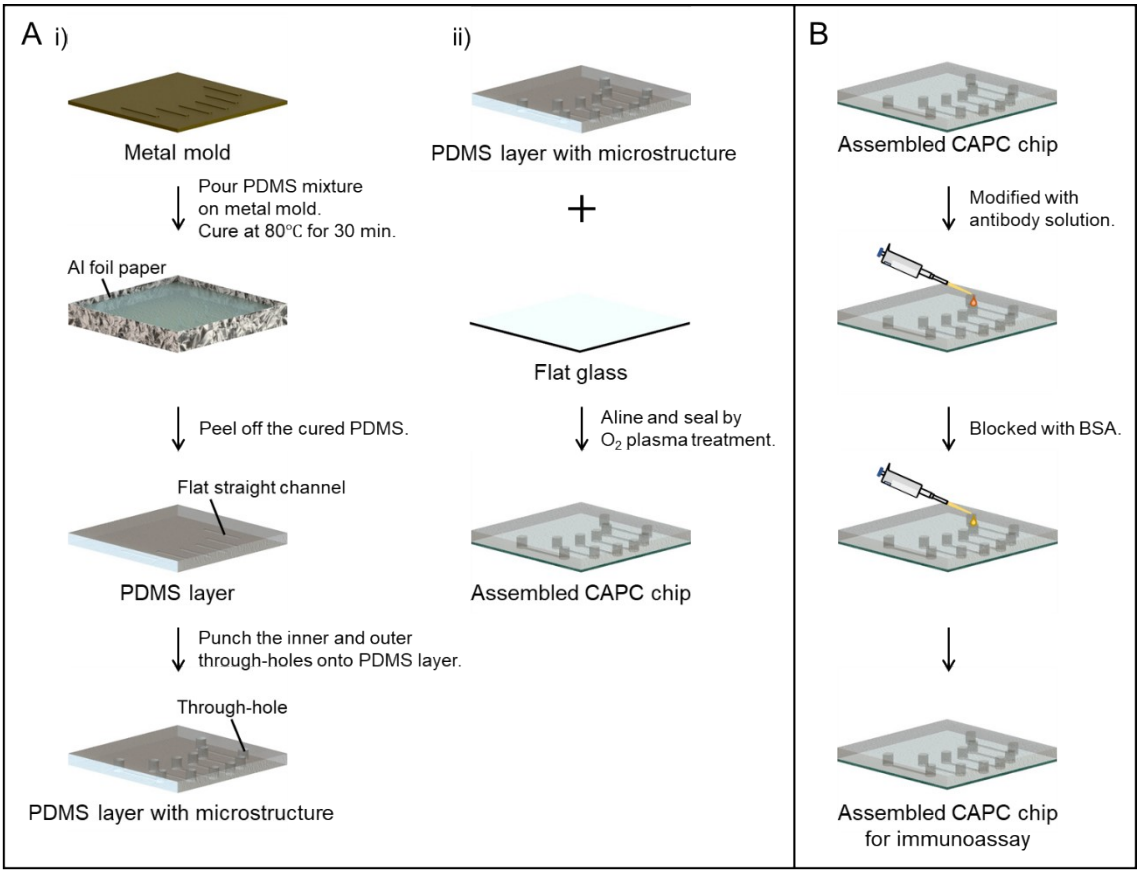

Fig. S3 The schematic diagram showing the fabrication process of the chip. (A) The fabrication process of the CAPC chip. i) The fabrication process of a PDMS layer with microstructure. ii) The assembling process of the CAPC chip. (B) The antibody-modified assembled CAPC chip for immunoassay.

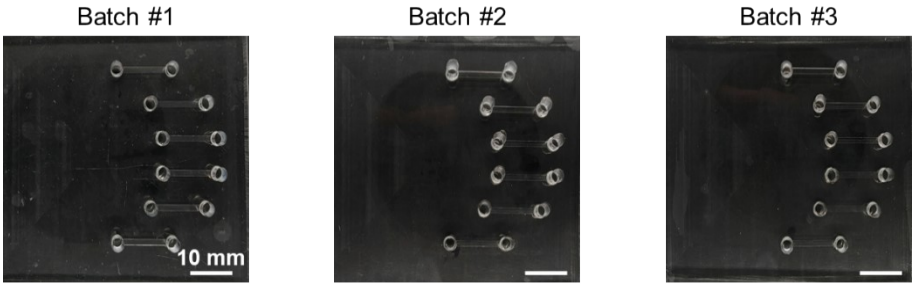

Fig. S4 The images of CAPC chips prepared in different batches.

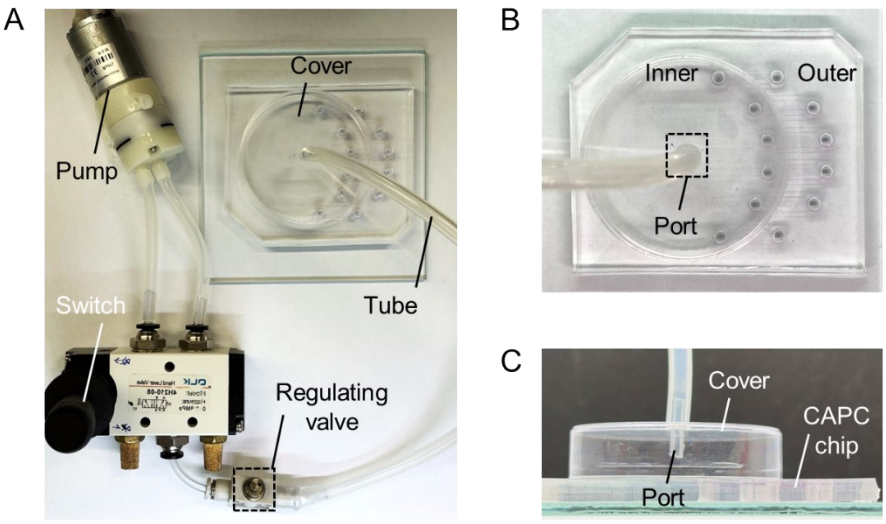

Fig. S5 The pressure control device used for controlling the reciprocating-flow of liquids in the channels of the CAPC chip. (A) The pressure control device, consisting of a bidirectional air pump, a tube and a pressure cover. (B) Top view of the pressure cover which sealed the six inner holes of the chip for applying pressure. (C) Side view of the pressure cover which sealed the six inner holes of the chip for applying pressure.

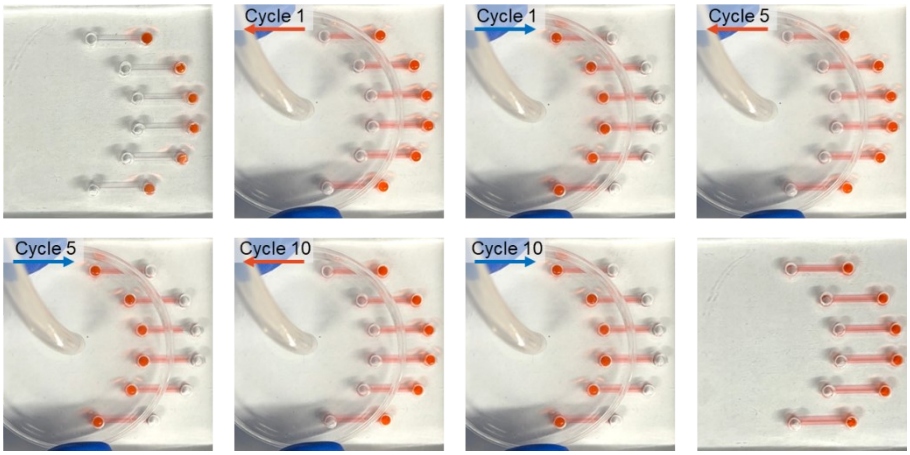

Fig. S6 Images illustrated the reciprocating-flow of red ink within the channels of CAPC chip over 10 cycles using the pressure control device.

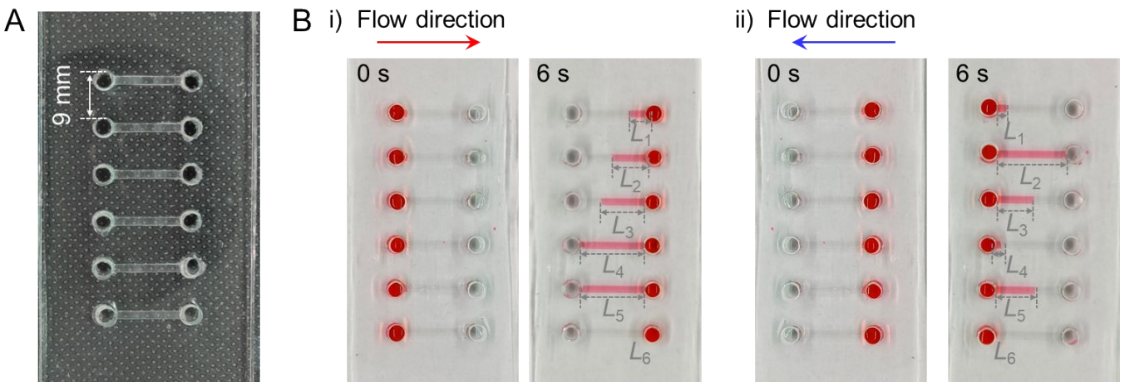

Fig. S7 The flow behavior of liquid in the channels of the linearly-aligned parallel channel chip (LAPC chip). (A) The top-view image of the LAPC chip. (B) The column lengths (L_i) of residual red ink in the channels of the LAPC chip at 0 s and 6 s in two flow directions.

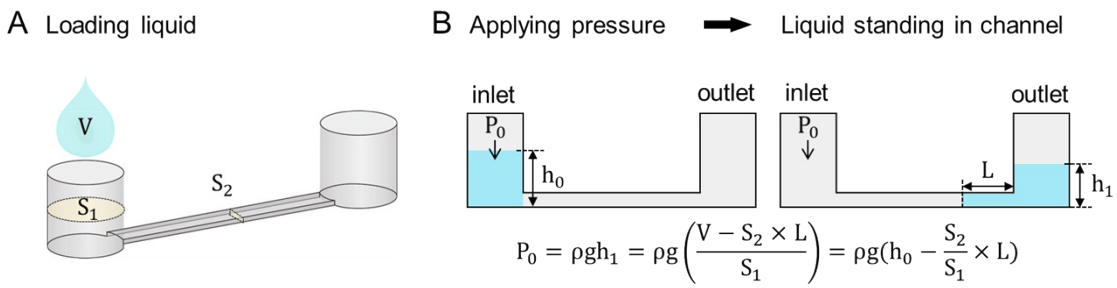

Fig. S8 Theoretical analysis of the relationship between the pressure applied at inlet and the column length of the residual liquid in the channel. (A) A single channel and its structure parameters. V is the volume of the loading liquid, S_1 is the cross-sectional area of the cylindrical through-hole, and S_2 is the cross-sectional area of the straight channel. (B) The diagram illustrates the process of the liquid flowing from the inlet to the outlet under applied pressure (P_0). The formula shows that the column length of the residual liquid in the channel (L) is influenced by P_0 after the flow, when S_1, S_2 and V are kept unchanged. h_0 and h_1 represent the height of the liquid column in the inlet and outlet, respectively.

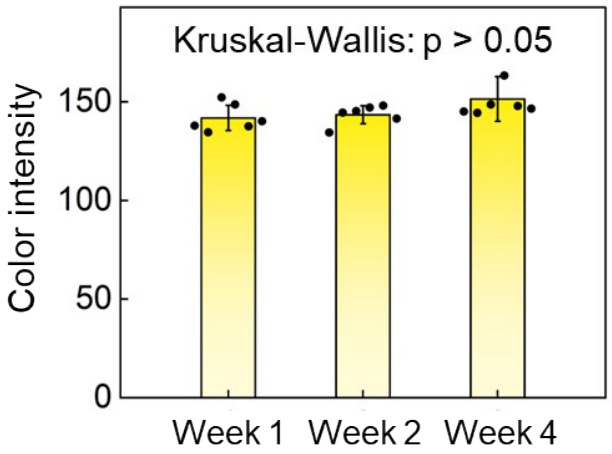

Fig. S9 Bar chart showed the colorimetric results of human IgG sample solution (37 μg/mL) using three CAPC chips from different fabrication batches after different storage durations.

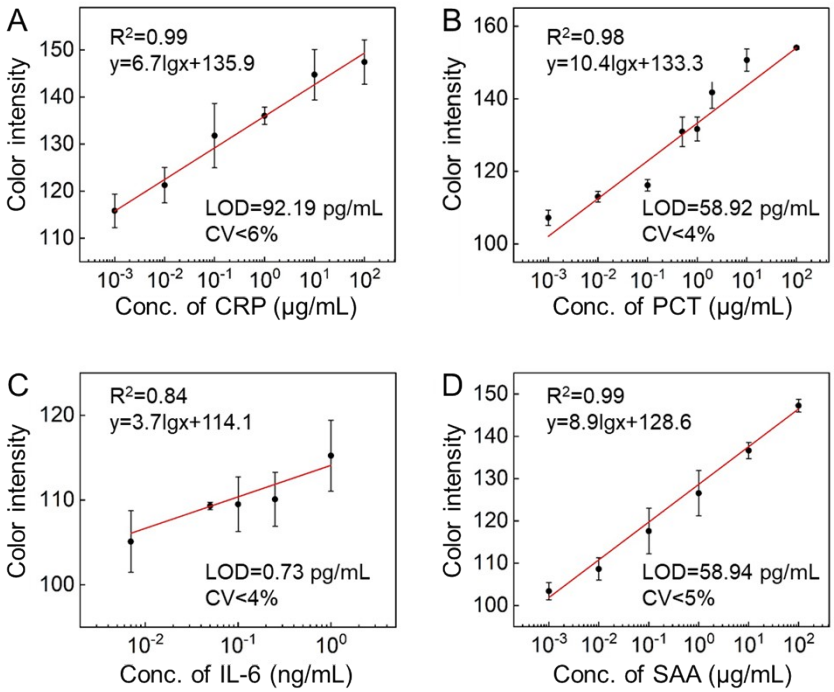

Fig. S10 The plot showed the relationship between the color intensities and the concentrations of (A) CRP, (B) PCT, (C) IL-6, (D)SAA, in the sample solutions.

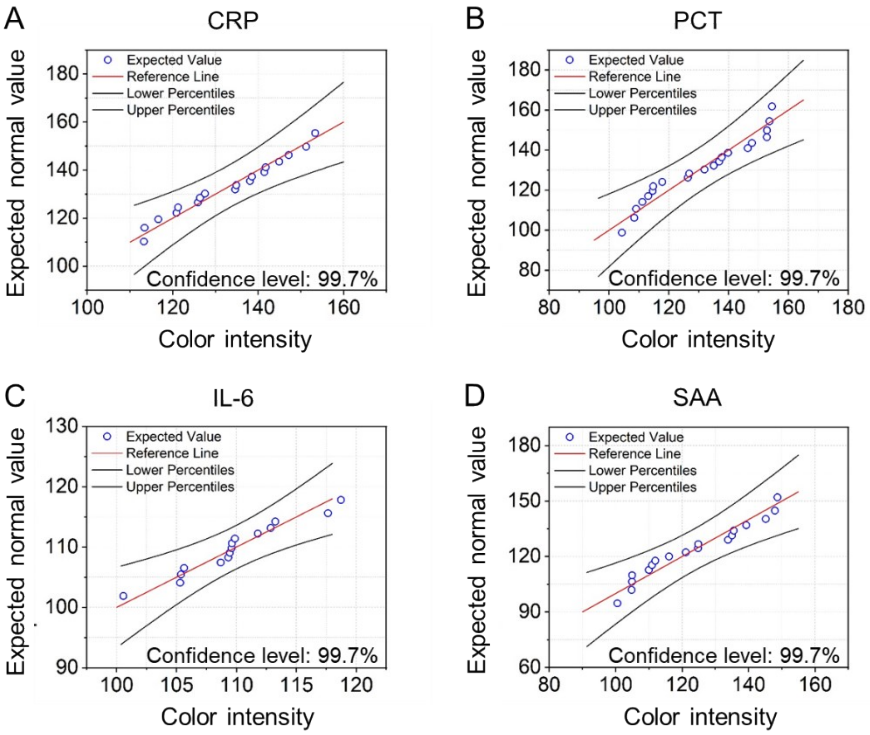

Fig. S11 Q-Q plots demonstrated the distribution of detection data for standard samples of four inflammatory markers: (A) CRP, (B) PCT, (C) IL-6, and (D) SAA.

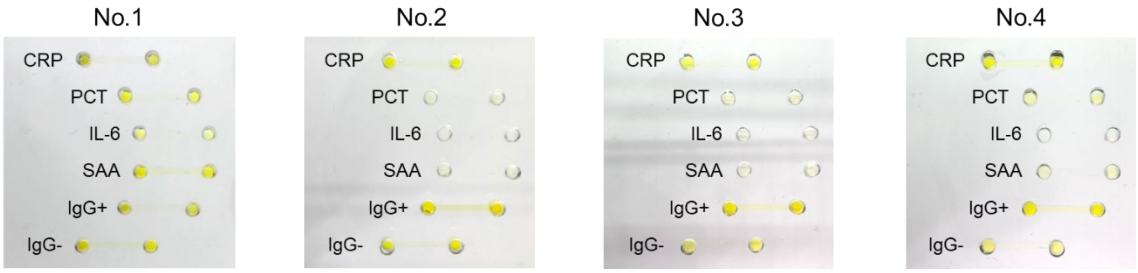

Fig. S12 Images of detection results of clinical serum samples obtained by CAPC chip.

Supplementary Tables

Table S1. The diagnostic thresholds of four inflammatory markers and LODs obtained by the CAPC chip proposed in this work.

Inflammatory markers	Diagnostic thresholds (g/mL)	LODs in this work (g/mL)
CRP	1.00E-5	9.22E-11
PCT	5.00E-10	5.89E-11
IL-6	7.00E-12	7.26E-13
SAA	1.00E-5	5.89E-11

Table S2. Representative application scenarios of combined detection of four inflammatory markers in clinical practice.

Scenario	Inflammatory Markers				Representative Application
	CRP	PCT	IL-6	SAA	
1	√			√	Testing for viral infections (CRP: 10-25 μg/mL, SAA: 10-100 μg/mL)[1, 2].
2	√			√	Testing for bacterial infections (CRP: > 50 μg/mL, SAA: 100-500 μg/mL)[1, 2].
3	√		√		Testing for viral infections such as influenza and coronavirus infections (e.g., COVID-19)[3, 4].
4	√	√	√	√	Testing for severe systemic bacterial infections such as sepsis and severe septicemia[5, 6].

Table S3. The qualitative detection results of clinical serum samples reported by the hospital and the qualitative detection results of clinical serum samples obtained by CAPC chip.

Sample No.	Inflammatory marker	Clinical detection results	CAPC chip detection results	Consistency
1	CRP	+	+	Yes
	PCT	+	+	
	IL-6	+	+	
	SAA	+	+	
2	CRP	-	-	Yes
	PCT	-	-	
	IL-6	-	-	
	SAA	-	-	
3	CRP	-	-	Yes
	PCT	-	-	
	IL-6	-	-	
	SAA	-	-	
4	CRP	-	-	Yes
	PCT	-	-	
	IL-6	-	-	
	SAA	-	-	

Table S4. Comparison between traditional immunoassay methods and CAPC chip-based ELISA method.

Method	LOD	Inflammatory markers detected in each assay	Detection speed (Detection time)
TIIA	1.0E-9 g/mL	CRP、SAA	Fast (10-15 min)
ELISA	1.0E-12 g/mL	CRP、PCT、IL-6、SAA	Slow (2-4 h)
CLIA	1.0E-12 g/mL	CRP、PCT、IL-6、SAA	Fast (20-30 min)
CAPC (this work)	1.0E-12 g/mL	CRP+PCT+IL-6+SAA	Fast (5 min）

Supplementary Movie

Movie S1. Movie demonstrating the process of ELISA detection using the CAPC chip.

Supplementary References

1. Chinese Society of Integrated Traditional and Western Laboratory Medicine, *Chin. J. Lab. Med.*, 2019, **42**, 186-192.
2. Infectious Diseases Society of China, *Chin. J. Tuberc. Respir. Dis.*, 2017, **40**, 243-257.
3. Y. D. Gao, M. Ding, X. Dong, J. J. Zhang, A. K. Azkur, D. Azkur, H. Gan, Y. L. Sun, W. Fu, W. Li, H. L. Liang, Y. Y. Cao, Q. Yan, C. Cao, H. Y. Gao, M. C. Brüggen, W. van de Veen, M. Sokolowska, M. Akdis and C. A. Akdis, *Allergy*, 2021, **76**, 428-455.
4. H. Han, Q. F. Ma, C. Li, R. Liu, L. Zhao, W. Wang, P. G. Zhang, X. H. Liu, G. S. Gao, F. Liu, Y. G. Jiang, X. M. Cheng, C. L. Zhu and Y. C. Xia, *Emerge. Microbes. Infec.*, 2020, **9**, 1123-1130.
5. S. Kibe, K. Adams and G. Barlow, *J. Antimicrob. Chemoth.*, 2011, **66**, ii33-ii40.
6. C. Pierrakos, D. Velissaris, M. Bisdorff, J. C. Marshall and J. L. Vincent, *Crit. Care*, 2020, **24**, 287.